

# Anionic amphiphile and phospholipid-induced conformational changes in human neutrophil flavocytochrome *b* observed by fluorescence resonance energy transfer

Ross M. Taylor, Thomas R. Foubert, James B. Burritt, Danas Baniulis,  
Linda C. McPhail, Algirdas J. Jesaitis\*

*Department of Microbiology, Montana State University, Bozeman, 109 Lewis Hall, Bozeman, MT 59717, USA*

Received 20 November 2003; received in revised form 8 March 2004; accepted 19 March 2004

Available online 17 April 2004

## Abstract

The integral membrane protein flavocytochrome *b* (Cyt *b*) comprises the catalytic core of the human phagocyte NADPH oxidase complex and serves to initiate a cascade of reactive oxygen species that participate in the elimination of infectious agents. Superoxide production by the NADPH oxidase complex has been shown to be specifically regulated by the enzymatic generation of lipid second messengers following phagocyte activation. In the present study, a Cyt *b*-specific monoclonal antibody (mAb 44.1) was labeled with Cascade Blue (CCB) and used in resonance energy transfer (RET) studies probing the effects of a panel of lipid species on the structure of Cyt *b*. The binding of CCB-mAb 44.1 to immunoaffinity-purified Cyt *b* was both highly specific and resulted in significant quenching of the steady state donor fluorescence. Titration of the CCB-mAb 44.1:Cyt *b* complex with the anionic amphiphile lithium dodecyl sulfate (LDS) resulted in a saturable relaxation of fluorescence quenching due to conformational changes in Cyt *b* at concentrations of the amphiphile required for maximum rates of superoxide production by Cyt *b* in cell-free assays. Similar results were observed for the anionic amphiphile arachidonic acid (AA), although no relaxation of fluorescence quenching was observed for arachidonate methyl ester (AA-ME). Saturable relaxation of fluorescence quenching was also observed with the anionic, 18:1 phospholipids phosphatidic acid (DOPA) and phosphatidylserine (DOPS), while no relaxation was observed upon addition of the neutral 18:1 lipids phosphatidylcholine (DOPC), phosphatidylethanolamine (DOPE) or diacylglycerol (DAG) at similar levels. Further examination of a variety of phosphatidic acid (PA) species demonstrated DOPA to both potently induce conformational changes in Cyt *b* and to cause more dramatic conformational changes than PA species with shorter, saturated acyl chains. The data presented in this study support the hypothesis that second messenger lipids, such as AA and PA, directly bind to flavocytochrome *b* and modulate conformational states relevant to the activation of superoxide production.

© 2004 Elsevier B.V. All rights reserved.

**Keywords:** Flavocytochrome *b*; Fluorescence; Structure; Phospholipid; Amphiphile

**Abbreviations:** AA, arachidonic acid; AA-ME, arachidonate methyl ester; AC-PQVRPI-CONH<sub>2</sub>, the peptide Pro-Gln-Val-Arg-Pro-Ile acetylated at the N-terminus and amidated at the C-terminus; CCB, Cascade Blue; Cyt *b*, human phagocyte flavocytochrome *b*; DAG, diacylglycerol; DDM, dodecylmaltoside; DOPA, 1,2-dioleoyl-*sn*-glycero-3-phosphate (18:1 PA); DOPC, 1,2-dioleoyl-*sn*-glycero-3-phosphocholine (18:1 PC); DOPE, 1,2-dioleoyl-*sn*-glycero-3-phosphoethanolamine (18:1 PE); DOPS, 1,2-dioleoyl-*sn*-glycero-3-[phospho-L-serine] (18:1 PS); DTT, dithiothreitol; EDTA, ethylenediaminetetraacetic acid; HEPES, *N*-[2-hydroxyethyl]piperazine-*N'*-[2-ethanesulfonic acid]; LDS, lithium dodecyl sulfate; mAb, monoclonal antibody; NADPH, nicotinamide adenine dinucleotide; PA, phosphatidic acid; PMSF, phenylmethylsulfonyl-fluoride; RET, resonance energy transfer; SDS-PAGE, sodium dodecyl sulfate polyacrylamide gel electrophoresis; WGA, wheat germ agglutinin

\* Corresponding author. Tel.: +1-406-994-4811; fax: +1-406-994-4926.

E-mail address: [umbaj@gemini.oscs.montana.edu](mailto:umbaj@gemini.oscs.montana.edu) (A.J. Jesaitis).

## 1. Introduction

In response to inflammatory stimuli, human phagocytes migrate to sites of infection and tissue injury where they are activated to release toxic proteins, hydrolytic enzymes and reactive oxygen species [1]. The generation of reactive oxygen species is initiated by the phagocyte NADPH complex, which catalyzes the one electron reduction of molecular oxygen to generate superoxide anion. The resulting superoxide anion serves as a precursor for the generation of toxic oxygen species such as hydrogen peroxide, hydroxyl radical and hypochlorous acid [2]. Flavocytochrome *b* (Cyt *b*) is a heterodimeric, integral membrane protein composed of a

heavily glycosylated, 570-amino-acid-residue subunit (gp91<sup>phox</sup>) and a 195-residue subunit (p22<sup>phox</sup>) that serves as the central, catalytic core of the NADPH oxidase complex [1,3]. Cyt *b* has been characterized as a flavoprotein [4–6] that coordinates two heme prosthetic groups [7–9] and contains all of the structural determinants required for transfer of metabolic electrons from NADPH across the plasma or phagosomal membrane for reduction of molecular oxygen [4,10]. Since reactive oxygen species have the capacity to damage healthy host tissue when generated in an inappropriate fashion, electron transfer through Cyt *b* is subject to strict spatial and temporal regulation. Following activation of phagocytes by inflammatory stimuli, the regulatory proteins p47<sup>phox</sup>, p67<sup>phox</sup>, p40<sup>phox</sup>, and Rac 1/2 translocate to the membrane and associate with flavocytochrome *b* to form the multicomponent, catalytically active NADPH oxidase complex [1,3,11].

Two prominent signal transduction events, namely the phosphorylation of oxidase components and the generation of lipid second messengers, have been shown to promote the assembly and activation of the NADPH oxidase complex following receptor-mediated activation of phagocytic cells [11,12]. Although second messenger lipids including arachidonic acid (AA), phosphatidic acid (PA) and diacylglycerol (DAG) have a well-defined role in signal transduction events that lead to phosphorylation of oxidase components [12], detailed investigation has also demonstrated the direct action of such biologically active lipids on both the membrane-bound and cytosolic components of the NADPH oxidase complex.

AA and PA have been shown to disrupt an interaction between the small G protein Rac and (Rho)GDI, allowing Rac to translocate from the cytosol to the membrane environment where it would be available for assembly into the NADPH oxidase complex [13]. In addition, a variety of observations have demonstrated the ability of AA to induce conformational changes in p47<sup>phox</sup> important for oxidase assembly and activation. Spectroscopic analysis of purified p47<sup>phox</sup> in the presence of the anionic amphiphiles lithium dodecyl sulfate (LDS) and AA demonstrated the ability of these agents to induce conformational changes analogous to those induced by *in vitro* phosphorylation by protein kinase C [14–16]. The conformational changes in p47<sup>phox</sup> brought about by treatment with anionic amphiphiles were both specific and occurred at levels that are required for maximal rates of superoxide production by the NADPH oxidase complex in *in vitro* cell-free assay systems. Further examination of the effects of AA on p47<sup>phox</sup> revealed that the conformational changes induced by this amphiphile serve to unmask the SH3 domains that mediate an interaction with a proline rich region in the small subunit of flavocytochrome *b* during oxidase assembly [17,18]. In addition, DAG and PA have been shown to promote assembly and activation of the NADPH oxidase complex [19–21], while PA alone has been demonstrated sufficient to induce conformational changes in p47<sup>phox</sup> [19]. How these amphipathic lipids are transported from membranes to such cytoplasmic targets

has yet to be resolved. An alternative view has been presented that suggests that anionic lipids predominantly serve as an ionic matrix in the membrane to attract, bind and facilitate the diffusion of Rac/p67<sup>phox</sup> complexes to Cyt *b* [22,23].

Evidence has also been generated to suggest that second messenger lipids interact directly with the integral membrane flavocytochrome *b* to promote assembly and/or activation of the NADPH oxidase complex. Following detergent extraction of pig neutrophil membranes, superoxide production was elicited upon addition of PA (in the absence of cytosolic oxidase factors) at levels similar to those observed when the detergent extracts were combined with cytosol and AA [24]. Similarly, PA was shown to support optimal superoxide production and enhanced binding of the flavin cofactor of purified flavocytochrome *b* in the absence of the cytosolic oxidase components [4,10]. In studies characterizing the effects of AA on flavocytochrome *b*, spectroscopic methods were used to demonstrate that this agent induced a change in the heme environment of both membrane-bound and detergent-solubilized Cyt *b* [25]. In addition, our group has recently employed CCB-labeled wheat germ agglutinin (WGA) as a donor for fluorescence resonance energy transfer (FRET) experiments demonstrating the ability of AA to induce structural changes in detergent-solubilized Cyt *b* [26]. Thus, evidence exists that the cytosolic oxidase components Rac and p47<sup>phox</sup> and the integral membrane component Cyt *b* may be directly regulated by physiologically generated lipid second messengers.

In the present study, we have extended our previous observations by Cascade Blue (CCB) labeling a Cyt *b*-specific, epitope-mapped monoclonal antibody (mAb) and using it as a more highly defined probe for investigating structural rearrangements of purified Cyt *b* by FRET [27,28]. Using this resonance energy transfer (RET) assay, a panel of phospholipids and amphiphiles were examined for the ability to induce conformational changes in detergent-solubilized flavocytochrome *b*.

## 2. Methods and materials

### 2.1. Materials

Dodecylmaltoside (DDM) was purchased from Fluka and octylglucoside, PMSF and DTT from Calbiochem. Cascade Blue acetyl azide and the anti-CCB rabbit polyclonal antibody were from Molecular Probes. LDS, AA, arachidonate methyl ester (AA-ME), sodium deoxycholate, chymostatin, the mammalian protease inhibitor cocktail (P8340), HEPES and Tris were obtained from Sigma. Protein A-Sepharose and GammaBind Plus-Sepharose beads were from Pharmacia; Centricon-30 concentrators from Millipore and the goat-anti mouse (H+L) alkaline phosphatase secondary antibody and Econo-Pac 10 DG

desalting columns (30 × 10 ml) from BioRad. ProSieve color molecular weight markers were purchased from BMA; Western blot developing reagents were purchased from Kirkegaard & Perry Laboratories and nitrocellulose (0.45 µm pore size) was from Schleicher & Schuell. The elution peptide AC-PQVRPI-CONH<sub>2</sub> (AC-, acetylation at the N-terminus of the elution peptide; -CONH<sub>2</sub>, amidation at the C-terminus of the elution peptide) was obtained from Macromolecular Resources. SDS, 0.2-µm polyethersulfone syringe filters (Whatman), acrylamide, bis-acrylamide, NaCl, NaH<sub>2</sub>PO<sub>4</sub>, KCl, EDTA, EGTA, NaN<sub>3</sub>, chloroform and HPLC grade methanol were from Fisher Scientific. The synthetic phospholipids 1,2-dioctanoyl-*sn*-glycero-3-phosphate (8:0 PA), 1,2-distearoyl-*sn*-glycero-3-phosphate (18:0 PA), 1,2-dioleoyl-*sn*-glycero-3-phosphate (18:1 PA), 1,2-dioleoyl-*sn*-glycero-3-[phospho-L-serine] (18:1 PS), 1,2-dioleoyl-*sn*-glycero-3-phosphocholine (18:1 PC), 1,2-dioleoyl-*sn*-glycero-3-phosphoethanolamine (18:1 PE), 1,2-dioctanoyl-*sn*-glycerol (8:0 DAG) and 1,2-dioleoyl-*sn*-glycerol (18:1 DAG) were purchased from Avanti Polar Lipids, Inc. The BCA protein determination kit and Reacti-Vial Small Reaction Vials (used for storing chloroform-solubilized lipids) were obtained from Pierce, while mAb 44.1 was produced in-house by standard hybridoma culture methods.

Absorption measurements were performed on an Agilent absorption spectrophotometer with quartz cuvettes obtained from the same supplier. Sonication was conducted with a 50 Sonic dismembrator probe sonicator from Fisher Scientific. Fluorescence spectroscopy was conducted using a Quanta-Master QM-1 fluorometer from Photon Technologies Inc., with the resulting data analyzed with software provided by the same manufacturer (Felix software ver. 1.1, 1996 PTI, Inc.). Cylindrical, UV-transparent micro-cuvettes (6-mm outside diameter) used for fluorescence measurements were obtained from Sienco. High-speed centrifugation of small-volume samples was conducted in a TLA-100 ultracentrifuge from Beckman, with centrifugation tubes and the TLA-100.2 rotor supplied from the same manufacturer.

## 2.2. Purification of mAb 44.1

Prior to labeling with CCB, mAb 44.1 was purified on a GammaBind affinity matrix. For purification, ~1 ml of GammaBind beads was first rinsed with 5 ml of 0.5 M acetic acid, pH 3.0, and then equilibrated by washing extensively with PBS (10 mM NaH<sub>2</sub>PO<sub>4</sub>/100 mM NaCl, pH 7.3). Hybridoma culture supernatant (500 ml) was then tumbled with the beads at 4 °C overnight and the column was successively washed with 20 ml PBS, followed by 10 ml PBS/0.5 M NaCl and finally 20 ml of 10 mM PBS. The antibodies were eluted from the GammaBind matrix by addition of 0.5 M acetic acid (pH 3.0), with 500-µl elution fractions collected directly into 400 µl of 1 M Tris, pH 9.0. Antibody eluted from the matrix was detected by absorption

spectroscopy, pooled and dialyzed against four changes of 2000 volumes of PBS at 4 °C. Following dialysis, antibody-containing solutions were concentrated to ~1 ml in a Centricon-30 concentrator and final protein concentration determined using the BCA method.

## 2.3. CCB labeling of mAb 44.1

mAb 44.1 was labeled under neutral pH conditions where acetyl azide compounds preferentially react with the N-termini of both the heavy and light chains of mouse IgG molecules [29]. For labeling, a 50-fold molar excess of CCB acetyl azide (dissolved as a 10 mM stock in methanol) was added to the antibody and the resulting mixture tumbled for 48 h at 4 °C. The reaction was terminated by addition of 100 mM hydroxylamine, pH 8.5, and free dye removed by chromatography on Bio-Rad P-10 desalting columns (equilibrated in PBS) with eluted antibody detected by absorption spectroscopy. The resulting, labeled antibody was pooled and further dialyzed against three changes of 2000 volumes of PBS. For determination of labeling stoichiometry, protein content was determined by the BCA method and CCB quantitated by absorbance spectroscopy using  $\epsilon_{400} = 31,400 \text{ M}^{-1} \text{ cm}^{-1}$  (obtained from Molecular Probes). This particular procedure resulted in a labeling stoichiometry of ~5.7:1 CCB/mAb 44.1. Since the absolute degrees of both fluorescence quenching and relaxation depend on the overall labeling stoichiometry (data not shown) and the particular residues that are covalently modified, results obtained with a single batch of CCB-labeled mAb 44.1, labeled as described above, were used when comparing relative relaxation of fluorescence quenching (Table 1) to enable direct comparison of the various lipids and amphiphiles.

Alternatively, production of CCB-mAb 44.1 with a similar labeling stoichiometry was carried out by addition of a 40-fold molar excess of CCB acetyl azide to the antibody (0.5 mg of mAb 44.1 in 400-µl PBS), with the resulting mixture tumbled for 1.5 h at room temperature. The reaction was terminated by addition of 75 mM Tris, pH 7.4 and free dye was removed by chromatography on Bio-Rad P-10 desalting columns (equilibrated in PBS) with eluted antibody detected by absorption spectroscopy. The resulting, labeled antibody was pooled and further dialyzed against 2000 volumes of PBS. Antibody labeled by this procedure was used primarily to obtain titration data with the various PA species and to analyze the effects of AA-ME on relaxation of fluorescence quenching induced by 10:0 PA and DOPA.

## 2.4. Purification of flavocytochrome b

Construction of the mAb 44.1 affinity matrix and immunoaffinity purification of Cyt *b* from neutrophil plasma membranes was conducted as previously described [9]. For removal of elution peptide following purification,

Table 1

Anionic amphiphiles and phospholipids induce conformational changes in detergent-solubilized flavocytochrome *b*

Lipid species examined	Relative relaxation of fluorescence quenching <sup>a</sup>	Apparent $K_d$ ( $\mu$ M)
Lithium dodecyl sulfate (LDS)	1.0	$51 \pm 14$ ( $n=6$ )
Arachidonic acid	0.85	$116 \pm 8$ ( $n=3$ )
18:1 Phosphatidic acid (DOPA)	0.83	$14 \pm 5$ ( $n=5$ )
10:0 Phosphatidic acid	0.68	$18 \pm 1$ ( $n=3$ )
18:1 Phosphatidylserine (DOPS)	0.39	not determined
8:0 Phosphatidic acid	0.34	$21 \pm 4$ ( $n=5$ )
18:1 Phosphatidylethanolamine (DOPE)	no relaxation observed	
18:1 Phosphatidylcholine (DOPC)	no relaxation observed	
18:1 Diacylglycerol	no relaxation observed	
8:0 Diacylglycerol	no relaxation observed	
Arachidonate methyl ester	no relaxation observed	

Following complex formation between CCB-mAb 44.1 and immunoaffinity-purified flavocytochrome *b*, the effects of a panel of lipid species on donor fluorescence were examined. The saturable relaxation of fluorescence quenching observed with various anionic amphiphiles and phospholipids represents conformational changes in flavocytochrome *b*.

<sup>a</sup> Since LDS gave the greatest observed relaxation, this value was given a value of 1 and the relaxation induced by other anionic lipids is reported relative to that observed with LDS. Results were obtained with a single batch of CCB-mAb 44.1 to facilitate direct comparison of the various lipids examined in this study. Analyses were conducted in at least triplicate and independent experiments with individual lipids were in agreement to within  $\pm 5\%$ .

Cyt *b*-containing fractions were concentrated to approximately 1 ml in a Centricon-50 concentrator and then dialyzed (with one change of buffer) against 1000 volumes of 50 mM  $K_2HPO_4$ /150 mM NaCl/1 mM EGTA/1 mM  $MgCl_2$  (pH 7.3) overnight at 4 °C. Prior to RET studies, Cyt *b* was centrifuged at  $108,000 \times g$  for 30 min in a TLA 100.2 rotor. Final Cyt *b* concentration was determined by absorption spectroscopy using  $\epsilon_{414} = 131,000 \text{ M}^{-1} \text{ cm}^{-1}$  [30].

## 2.5. Preparation of lipid stock solutions

Phospholipids, DAGs, AA and AA-ME were stored in chloroform at  $-20$  °C in sealed containers after briefly purging with argon. For preparation of working stock solutions, the appropriate amount of lipid was transferred to a borosillate glass tube and samples were vortexed under a stream of argon for removal of the chloroform. Lipids were resuspended to a final concentration of 2.5 mM by addition of an appropriate amount of filtered PBS/1% DDM and then dispersed by vortexing and brief probe sonication. The LDS and deoxycholate working solutions (2.5 mM) were prepared in PBS and filtered prior to use. All lipid working solutions were used fresh on the day of preparation.

## 2.6. Fluorescence resonance energy transfer studies

Solutions containing Cyt *b* and CCB-labeled antibodies were kept on ice prior to use while lipid stock solutions were stored at room temperature. Fluorescence measurements were conducted in continuously stirred, UV-transparent microcuvettes at room temperature with the excitation monochromator set at 376 nm and the emission monochromator set at 418 nm. The slit width for both monochromators was set at 2 nm, corresponding to 4- and 8-nm bandpass for the excitation and emission monochromators, respectively. Experimental concentrations of both CCB-mAb 44.1 and Cyt *b* were well below the level where any significant inner-filter effects would occur ( $A_{376} < 0.001$  AU for both CCB and Cyt *b*).

For fluorescence measurements, CCB-labeled antibody was diluted to 10 nM in PBS/0.03% DDM and filtered prior to use. After background fluorescence had been established with a filtered solution of PBS/0.03% DDM (in a separate cuvette), fluorescence of the labeled antibody was monitored for a short time prior to addition of other agents. Flavocytochrome *b* (typically 30 nM final) was added directly to the stirred microcuvette and fluorescence emission monitored until a steady state was achieved. Lipids and amphiphiles were then added directly to the microcuvette and fluorescence emission again monitored until a steady state was achieved. All experiments were conducted at least in triplicate and were generally reproducible to within  $\pm 5\%$  of the observed relaxation of fluorescence quenching when comparing a single batch of CCB-mAb 44.1. For analysis of the effects of AA-ME on the relaxation of fluorescence quenching induced by 10:0 PA and DOPA, AA-ME was added to the CCB-mAb 44.1 stock solution prior to the addition of Cyt *b* and anionic lipids.

Titration curves were obtained for determination of apparent dissociation constants for the anionic lipids AA, LDS, 8:0 PA, 10:0 PA and DOPA, with the absolute values of fluorescence change fit to a one-phase exponential association curve by nonlinear regression using the equation  $Y = Y_{\max}(1 - e^{-kx})$ , where  $Y_{\max}$  represents fluorescence at saturation of the quenching effect. All curve-fitting analyses were performed using GraphPad Prism version 3.02 software. Apparent  $K_d$  values for the various anionic lipids are provided with the understanding that such lipids may partition and disperse into DDM micelles to various extents, creating an undefined effective local concentration for Cyt *b*.

## 2.7. Control experiments ensuring that lipids do not dissociate the CCB-mAb 44.1:Cyt *b* complex, do not alter donor fluorescence and do not alter the Cyt *b* heme spectrum

To ensure that the various lipids and amphiphiles did not significantly dissociate the CCB-mAb 44.1:Cyt *b* complex, immunoprecipitation experiments were conducted and Cyt *b* content of the resulting supernatant fractions assessed by absorption spectroscopy. For immunoprecipitation experi-



ments, Cyt *b* (75 nM) and CCB-mAb 44.1 (50 nM) were added to PBS/0.03% for a final volume of 1.65 ml and rotated at room temperature for 5 min. Following this incubation, 200  $\mu$ l of the above mixture was added to 50  $\mu$ l of packed GammaBind Plus-Sepharose beads (that had been previously equilibrated in PBS) and the resulting mixtures rotated for 15 min at room temperature. Lipids and amphiphiles examined in RET studies were next added to the above samples at a final concentration of 150  $\mu$ M and the resulting samples rotated for 10 min at room temperature. The GammaBind beads were then pelleted by brief centrifugation and resulting supernatant fraction analyzed for Cyt *b* content by absorption spectroscopy. Total Cyt *b* in these samples was determined by a similar experiment where protein was incubated with the GammaBind beads in the absence of CCB-mAb 44.1.

To ensure that the phospholipids and amphiphiles examined in this study did not significantly alter the steady state fluorescence of CCB-mAb 44.1, donor fluorescence was monitored following addition of these agents in the absence of Cyt *b*. To ensure that the phospholipids and amphiphiles examined in this study did not significantly alter the Cyt *b* Soret absorbance band, immunoaffinity-purified Cyt *b* was exposed to these agents (150  $\mu$ M) for 5 min at room temperature and then analyzed by absorption spectroscopy.

### 3. Results

#### 3.1. CCB-mAb 44.1 is a specific donor for RET studies with Cyt *b* heme acceptors

In the interest of generating a defined, site-specific probe for exploring conformational changes in flavocytochrome *b* by RET methods, the Cyt *b*-specific mAb 44.1 [31] was labeled with the fluorescent donor CCB [32]. Covalent modification of mAb 44.1 under the outlined conditions resulted in a labeling stoichiometry of  $\sim 5.7$  mol CCB:1

mol mAb 44.1 (Fig. 1A). Western blot analysis using an anti-CCB polyclonal antibody demonstrated the incorporation of label on both the heavy and light chains of mAb 44.1 (data not shown).

To examine both the activity of mAb 44.1 following CCB modification and the utility of this reagent for RET measurements, the fluorescence emission of CCB-mAb 44.1 (10 nM) was monitored following addition of immunoaffinity-purified Cyt *b* (10 nM final Cyt *b* in the fluorescence cuvette following each addition; Ref. [9] shows a representative SDS-PAGE gel demonstrating the high degree of purity of Cyt *b* used in this study). As observed in Fig. 1B, addition of Cyt *b* resulted in quenching of CCB fluorescence with

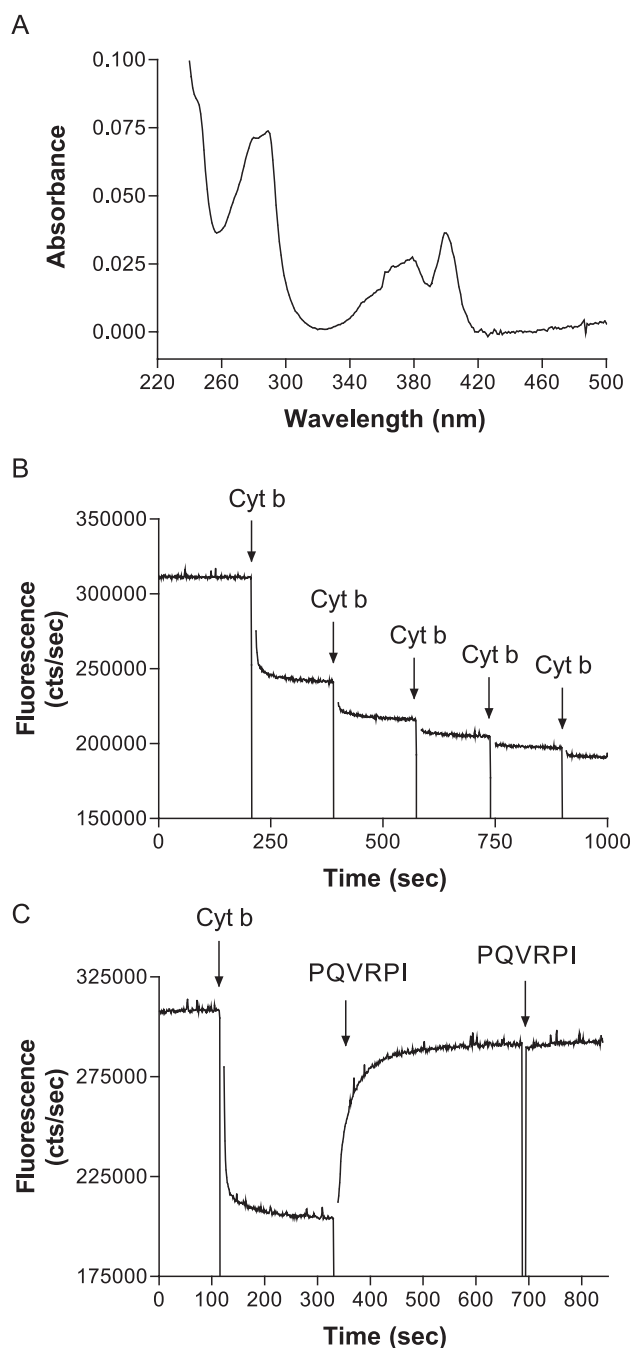


Fig. 1. Fluorescence quenching from RET following the specific and saturable association of CCB-mAb 44.1 and immunoaffinity-purified flavocytochrome *b*. Following covalent modification of the epitope-mapped, Cyt *b*-specific mAb 44.1 with Cascade Blue acetyl azide, the utility of this fluorescence donor was examined in RET studies with immunoaffinity-purified flavocytochrome *b*. (A) The absorption spectrum of CCB-mAb 44.1 (20-fold dilution of stock solution) showing the absorption band at 400 nm used to calculate the CCB content of labeled fractions. Protein content of this fraction was estimated by the BCA method for determination of a labeling stoichiometry of  $\sim 5.7$ :1 CCB/mAb 44.1 (molar ratio). (B) The saturable decrease in the steady state fluorescence of CCB-mAb 44.1 (10 nM CCB-mAb final representing 20 nM Cyt *b* binding sites) resulting from complex formation following equimolar additions of immunoaffinity-purified flavocytochrome *b* (10 nM Cyt *b* in the fluorescence cuvette at each addition). Arrows indicate the timepoints at which Cyt *b* was added to the fluorescence cuvette containing CCB-mAb 44.1. (C) The relaxation of fluorescence quenching observed following addition of the epitope mimicking peptide, AC-PQVRPI-CONH<sub>2</sub>. Arrows indicate the addition of both Cyt *b* (30 nM final) and AC-PQVRPI-CONH<sub>2</sub> (250  $\mu$ M additions) to the fluorescence cuvette containing CCB-mAb 44.1 (10 nM).

~ 90% of the total quenching observed following addition of a twofold molar excess of Cyt *b* (40 nM) relative to the total concentration of CCB-mAb 44.1 binding sites (10 nM CCB-mAb 44.1 represents a 20 nM concentration of binding sites assuming that both variable regions associate with Cyt *b*). Western blot analysis confirmed that the activity of mAb 44.1 was not appreciably compromised following covalent modification (data not shown).

Previous studies have shown the epitope-mimicking peptide AC-PQVRPI-CONH<sub>2</sub> to potentially dissociate the Cyt *b*-mAb 44.1 complex [31]. To confirm the specificity of the complex formed between purified Cyt *b* and CCB-mAb 44.1 under the conditions of our RET measurements, the effects of AC-PQVRPI-CONH<sub>2</sub> on the observed fluorescence quenching were investigated. Addition of the epitope-mimicking peptide (250  $\mu$ M) resulted in disruption of the Cyt *b*-antibody complex as judged by the rapid relaxation of fluorescence quenching (Fig. 1C). A subsequent addition of peptide had minimal effect, indicating saturation of the observed fluorescence relaxation. Specificity of the interaction between CCB-mAb 44.1 and Cyt *b* was also demonstrated by the lack of fluorescence quenching observed upon addition of Cyt *b* in the presence of a 25-fold molar excess of unlabeled antibody (data not shown).

### 3.2. Conformational changes in DDM-solubilized flavocytochrome *b* are induced by the anionic amphiphiles LDS and AA

The anionic amphiphiles LDS and AA have long been used for activation of the NADPH oxidase complex in cell-free assay systems [33,34] and previous studies have demonstrated the ability of these agents to induce structural changes in flavocytochrome *b* [25,26]. To characterize the effects of these anionic amphiphiles in our RET system, LDS and AA were introduced into the system following formation of the CCB-mAb 44.1:Cyt *b* complex. Fig. 2A shows the relaxation in fluorescence quenching observed

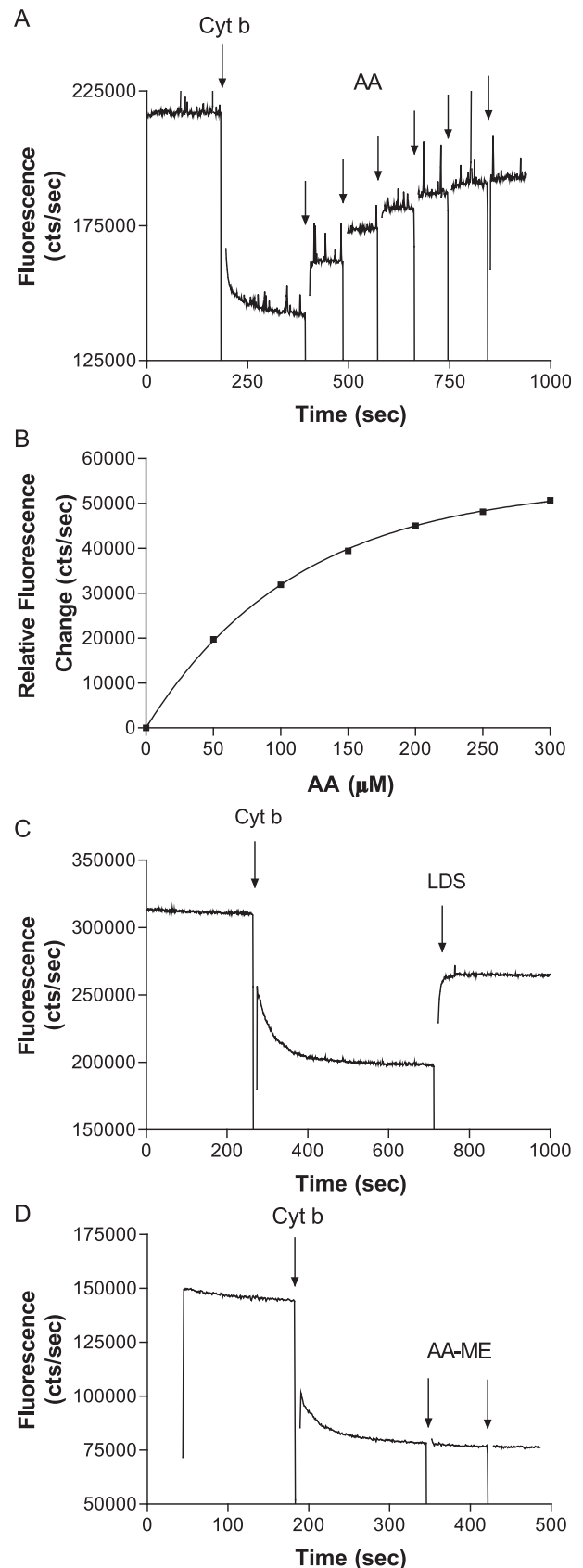


Fig. 2. The anionic amphiphiles AA and LDS induce conformational changes in immunoaffinity-purified flavocytochrome *b*. After formation of the CCB-mAb 44.1:Cyt *b* complex, steady state fluorescence was monitored following addition of AA, LDS or AA-ME. (A) The saturable relaxation of fluorescence quenching observed when AA was added the CCB-mAb 44.1:Cyt *b* complex. Arrows indicate the addition of both Cyt *b* (30 nM final) and AA (50  $\mu$ M additions) to the fluorescence cuvette containing CCB-mAb 44.1 (10 nM). (B) Representative analysis of titration curves obtained with the anionic amphiphile AA. The apparent  $K_d$  for AA was calculated to be  $116 \pm 8$   $\mu$ M ( $n=3$ ), while similar analysis of the anionic amphiphile LDS (data not shown) indicated an apparent  $K_d$  of  $51 \pm 14$   $\mu$ M ( $n=6$ ). (C) The relaxation of fluorescence quenching observed when LDS was added the CCB-mAb 44.1:Cyt *b* complex. Arrows indicate the addition of both Cyt *b* (30 nM final) and LDS (100  $\mu$ M final) to the fluorescence cuvette containing CCB-mAb 44.1 (10 nM). The observed relaxation in fluorescence quenching was fully saturated at this level of LDS. (D) The lack of observable fluorescence quenching when AA-ME was added the CCB-mAb 44.1:Cyt *b* complex. Arrows indicate the addition of both Cyt *b* (30 nM final) and AA-ME (100  $\mu$ M additions) to the fluorescence cuvette containing CCB-mAb 44.1 (10 nM).

when increasing amounts of AA (50  $\mu$ M additions) were added to the CCB-mAb 44.1:Cyt *b* complex. The effect of AA was saturable and resulted in maximal relaxation of fluorescence quenching at levels commonly employed for maximal activation of the NADPH oxidase complex in cell-free assays ( $\sim 150$   $\mu$ M AA). Analysis of titration curves (Fig. 2B) indicated an apparent  $K_d$  of  $116 \pm 8$   $\mu$ M ( $n=3$ ) for AA under these assay conditions. Similar results were observed for the anionic amphiphile LDS, with maximal relaxation of fluorescence quenching occurring when this agent was added at  $\sim 100$   $\mu$ M (Fig. 2C). Analysis of titration curves indicated an apparent  $K_d$  of  $51 \pm 14$   $\mu$ M ( $n=6$ ) for LDS under these assay conditions (data not shown). In contrast to LDS and AA, no significant relaxation of fluorescence quenching was observed upon addition of similar concentrations of the compound AA-ME (Fig. 2D) or the anionic amphiphile deoxycholate (data not shown). Table 1 summarizes results obtained with LDS, AA and AA-ME.

### 3.3. Anionic amphiphiles do not dissociate the CCB-mAb 44.1:Cyt *b* complex, do not perturb CCB-mAb 44.1 fluorescence and do not alter the Cyt *b* absorbance spectrum

To rule out a trivial explanation of our observed RET results, control experiments were conducted to explore effects of the above agents on: (1) the baseline fluorescence of CCB-mAb 44.1; (2) the association state of the CCB-mAb 44.1:Cyt *b* complex; and (3) the Soret absorbance spectrum of affinity-purified Cyt *b*. Fig. 3A shows no observable change in the fluorescence emission of CCB-mAb 44.1 following addition of AA at levels which resulted in significant relaxation of fluorescence quenching of the CCB-mAb 44.1:Cyt *b* complex. Similar results were observed with both LDS and AA-ME (data not shown) and rule out the possibility that the observed relaxation of fluorescence quenching in the presence of Cyt *b* was due to direct effects of these amphiphiles on the labeled antibody itself. To ensure that the amphiphiles AA and LDS did not dissociate the CCB-mAb 44.1:Cyt *b* complex (resulting in physical separation of the fluorescence donor–acceptor pair), immunoprecipitation experiments were conducted in the presence and absence of these agents. Such experiments indicated that addition of AA (Fig. 3B), LDS and AA-ME (data not shown) resulted in no significant dissociation of the CCB-mAb 44.1:Cyt *b* complex, similarly ruling out this possible effect as a cause for the observed relaxation of fluorescence quenching in these RET studies. Since an alteration in the spectral overlap between CCB and the Cyt *b* Soret spectrum might also account for the observed relaxation in fluorescence quenching, the effects of AA, LDS and AA-ME on the Cyt *b* Soret absorbance spectrum were characterized. Fig. 3C demonstrates that AA has no effect on the nature of the Cyt *b* Soret band, eliminating such effects as a possible explanation for the results ob-

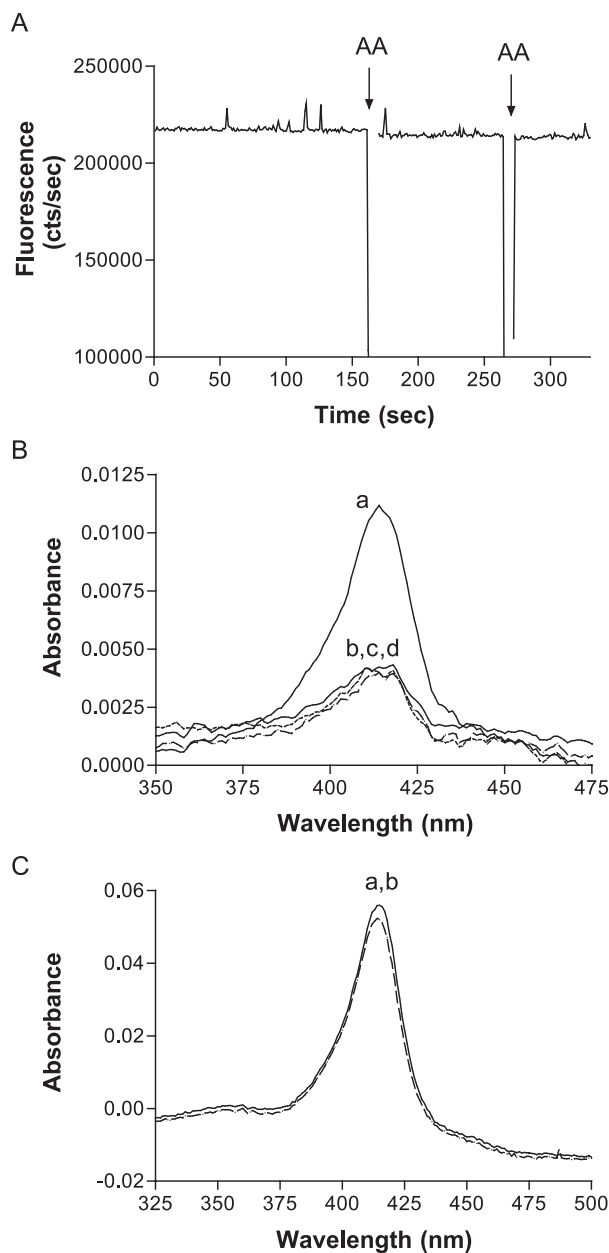


Fig. 3. Control experiments confirming that amphiphile-induced relaxation of fluorescence quenching results from conformational changes in flavocytochrome *b*. The following control experiments were conducted to examine the effects of AA, LDS and AA-ME on various components of the RET assay. (A) AA (100  $\mu$ M additions) has no effect on the steady state fluorescence of CCB-mAb 44.1. Similar results were observed for LDS and arachidonate ethyl ester. (B) Addition of AA (150  $\mu$ M final) does not lead to appreciable dissociation of the CCB-mAb 44.1:Cyt *b* complex as measured by immunoprecipitation of Cyt *b*. Curve a (—), supernatant absorption following incubation of Cyt *b* and GammaBind beads in the absence of CCB-mAb 44.1 (total Cyt *b*); Curve b (—), supernatant absorption following immunoprecipitation of Cyt *b* by CCB-mAb 44.1; Curve c (···), supernatant absorption following immunoprecipitation of Cyt *b* by CCB-mAb 44.1 in the presence of AA; Curve d (— — —), supernatant absorption following immunoprecipitation of Cyt *b* by CCB-mAb 44.1 in the presence of DOPA (see Results, Fig. 5). Similar results were obtained for LDS and AA-ME. (C) The Soret absorption spectrum of immunoaffinity-purified Cyt *b* (Curve a; —) is not altered in the presence of 150  $\mu$ M AA (Curve b; — — —). Similar results were obtained for LDS and AA-ME.

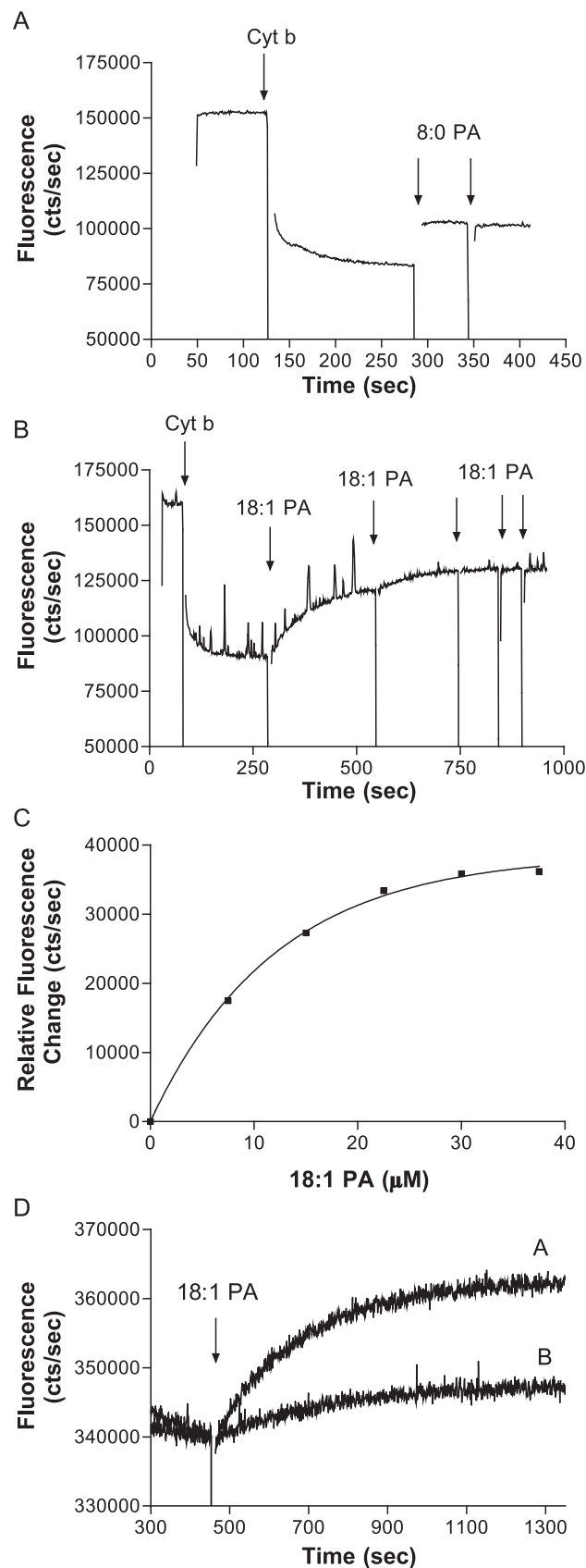
served in our RET studies. Similar results were obtained for both LDS and AA-ME (data not shown).

In light of results obtained in the above control experiments, we conclude that the observed relaxation in fluorescence quenching indicates an increase in the distance between the fluorescence donor (CCB) and the Cyt *b* heme prosthetic groups and/or a significant alteration of the relative orientation of the Cyt *b* heme prosthetic groups and CCB. Consistent with previous studies [25,26], these results demonstrate the ability of anionic amphiphiles to induce conformational changes in flavocytochrome *b*. The lack of relaxation in fluorescence quenching in the presence of AA-ME is supported by studies demonstrating the inability of this agent to induce conformational changes in Cyt *b* [25,26].

### 3.4. Structural changes in DDM-solubilized flavocytochrome *b* are induced by PA species

The involvement of both phospholipase D and PA in the regulation of the NADPH oxidase complex [12,21] raises the possibility that, in addition to previously characterized roles in signal transduction, PA also acts directly at the level of flavocytochrome *b*. To characterize the effects of PA on the structure of flavocytochrome *b*, different PA species were introduced into the RET assay following formation of the CCB-mAb 44.1:Cyt *b* complex. Fig. 4A and B demonstrates the observed relaxation in fluorescence quenching when the CCB-mAb 44.1:Cyt *b* complex was exposed to 8:0 PA (100  $\mu$ M additions) or DOPA (18:1 PA; 25  $\mu$ M additions). Although a kinetically slower process is observed with the long-chain PA species, a greater degree of relaxation was achieved with DOPA than with its 8:0 analog. Similar analysis with 10:0 PA demonstrated that this lipid also resulted in relaxation of the observed fluorescence quenching (data not shown), while the phospholipid 18:0 PA proved too insoluble to obtain consistent

Fig. 4. PA species induce conformational changes in immunoaffinity-purified flavocytochrome *b*. Following formation of the CCB-mAb 44.1:Cyt *b* complex, steady state fluorescence was monitored following addition of 8:0 PA or DOPA (18:1 PA). (A) The relaxation of fluorescence quenching observed when the CCB-mAb 44.1:Cyt *b* complex is exposed to 8:0 PA. Arrows indicate the addition of both Cyt *b* (30 nM final) and 8:0 PA (100  $\mu$ M additions) to the fluorescence cuvette containing CCB-mAb 44.1 (10 nM). (B) The saturable nature of the relaxation of fluorescence quenching observed when the CCB-mAb 44.1:Cyt *b* complex is titrated with DOPA. Arrows indicate the addition of both Cyt *b* (30 nM final) and DOPA (25  $\mu$ M additions) to the fluorescence cuvette containing CCB-mAb 44.1 (10 nM). (C) Representative analysis of titration curves obtained with the anionic phospholipid DOPA. The apparent  $K_d$  for DOPA was calculated to be  $14 \pm 5 \mu$ M ( $n=5$ ), while similar analysis of the anionic phospholipids 8:0 PA and 10:0 PA (data not shown) indicated an apparent  $K_d$  of  $21 \pm 4 \mu$ M ( $n=5$ ) and  $18 \pm 1 \mu$ M ( $n=3$ ), respectively. (D) The relaxation of fluorescence quenching observed when the CCB-mAb 44.1:Cyt *b* complex is exposed to 18:1 PA (10 nM final) in the absence (Curve A) and presence (Curve B) of a 20-fold molar excess of AA-ME. Arrow indicates the addition of DOPA to the fluorescence cuvette following formation of the CCB-mAb 44.1:Cyt *b* complex.





energy transfer measurements. Analysis of titration curves indicated apparent  $K_d$  values of  $21 \pm 4 \mu\text{M}$  ( $n=5$ ) for 8:0 PA,  $18 \pm 1 \mu\text{M}$  ( $n=3$ ) for 10:0 PA and  $14 \pm 5 \mu\text{M}$  for DOPA (Fig. 4C) under these assay conditions. Table 1 summarizes results obtained with 8:0 PA, 10:0 PA and DOPA.

Since AA-ME has previously been shown to competitively inhibit both anionic amphiphile-induced activation of the NADPH oxidase complex and conformational changes in Cyt *b* [25,26], the effects of AA-ME on PA-induced conformational changes in Cyt *b* were also examined in this study. In these experiments, the effects of 10:0 PA and DOPA (10  $\mu\text{M}$  final) on the CCB-mAb 44.1:Cyt *b* complex were analyzed in the presence and absence of a 20-fold molar excess of AA-ME (200  $\mu\text{M}$  final). Results obtained under these experimental conditions indicated that the presence AA-ME diminishes the relaxation of fluorescence quenching induced by both 10:0 PA ( $20 \pm 2\%$  relaxation ( $n=5$ ) in the absence of AA-ME;  $12 \pm 2\%$  relaxation ( $n=6$ ) in the presence of AA-ME) and DOPA ( $32 \pm 6\%$  relaxation ( $n=6$ ) in the absence of AA-ME;  $10 \pm 3\%$  relaxation ( $n=6$ ) in the presence of AA-ME).

Similar to results obtained with the anionic amphiphiles, control experiments indicated that DOPA: (1) had no significant effect on the fluorescence emission of CCB-mAb 44.1 (Fig. 5A); (2) did not appreciably dissociate the CCB-mAb 44.1:Cyt *b* complex (see Fig. 3B); and (3) had little effect on the nature of the Cyt *b* Soret absorbance spectrum (Fig. 5B). Similar results were obtained in control experiments conducted with 8:0 PA and 10:0 PA (data not shown). The above results indicate that the various PA species examined were able to directly induce conformational changes in purified flavocytochrome *b* in a structure-specific fashion.

### 3.5. Structural changes in DDM-solubilized flavocytochrome *b* are specifically induced by anionic phospholipids

The observation that a variety of PA species were capable of inducing conformational changes in flavocytochrome *b* raises the question of whether such effects are lipid-species-specific or simply a general property of phospholipids under such assay conditions. To examine the specificity of phospholipids for inducing structural changes in Cyt *b*, a panel of synthetic 18:1 phospholipids with different headgroups was examined in our RET system. Fig. 6A–D shows the effects of the phospholipids DOPA, DOPS, DOPC and DOPE when added to the CCB-mAb 44.1:Cyt *b* complex. Such analysis demonstrates that exposure to DOPA results in the most dramatic relaxation of fluorescence quenching (Fig. 6A), while the phospholipid DOPS induces a more modest conformation change in Cyt *b* (Fig. 6B) as determined by this specific assay system. In contrast, addition of similar concentration of either DOPC (Fig. 6C) or DOPE (Fig. 6D) resulted in no observable relaxation of fluorescence quenching. Table 1 summarizes

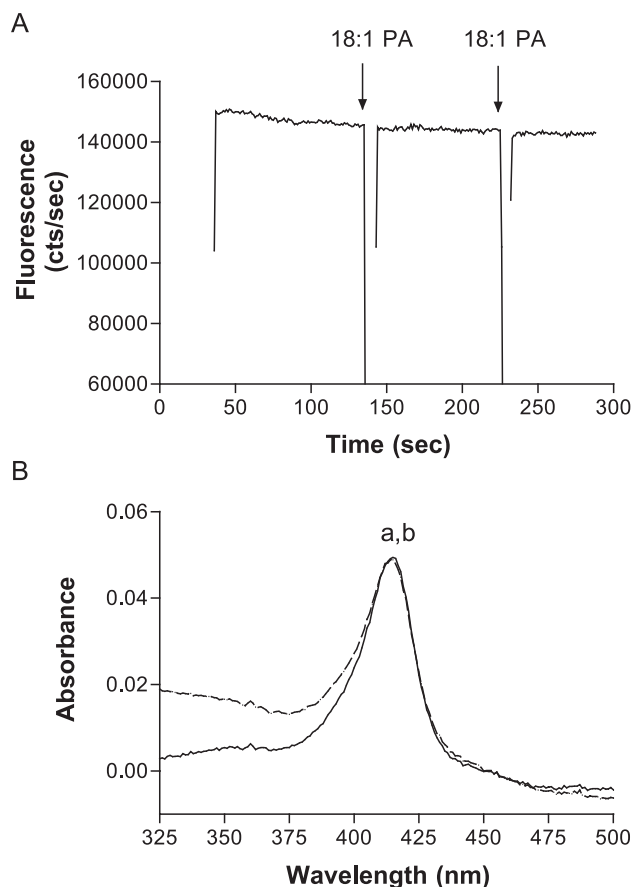


Fig. 5. Control experiments confirming that PA-induced relaxation of fluorescence quenching results from conformational changes in flavocytochrome *b*. The following control experiments were conducted to examine the effects of PA species on various components of the RET assay. (A) Demonstration that DOPA (100  $\mu\text{M}$  additions) has no effect on the steady state fluorescence of CCB-mAb 44.1. Similar results were observed for all phospholipids and DAGs examined in this study. (B) The Soret absorption spectrum of immunoaffinity-purified Cyt *b* (Curve a; —) is not altered in the presence of 150  $\mu\text{M}$  DOPA (Curve b; - - -). Similar results were obtained for all lipids examined in this study. See Fig. 3B for a demonstration that DOPA (150  $\mu\text{M}$  final) does not lead to appreciable dissociation of the CCB-mAb 44.1:Cyt *b* complex. Similar results were obtained for all phospholipids and DAGs examined in this study.

results obtained with the 18:1 phospholipids DOPA, DOPS, DOPC and DOPE.

Since previous reports have demonstrated the ability of both short-chain PA and short-chain DAG to individually support modest activation of the NADPH oxidase complex [35], the ability of both 8:0 and 18:1 DAG to induce conformational changes in Cyt *b* was also examined. In contrast to results obtained with PA species, exposure of the CCB-mAb 44.1:Cyt *b* complex to similar levels of 8:0 DAG (data not shown) or 18:1 DAG (Fig. 6E) resulted in no significant relaxation of fluorescence quenching. Previous observations that a combination of short-chain PA and DAG species resulted in synergistic activation of superoxide production [35] led us to examine the effects of DAG on titration curves conducted with DOPA. In these experi-

ments, prior exposure of the CCB-mAb 44.1:Cyt *b* complex to 100  $\mu$ M levels of either 8:0 or 18:1 DAG resulted in no significant alteration of the titration curve conducted with

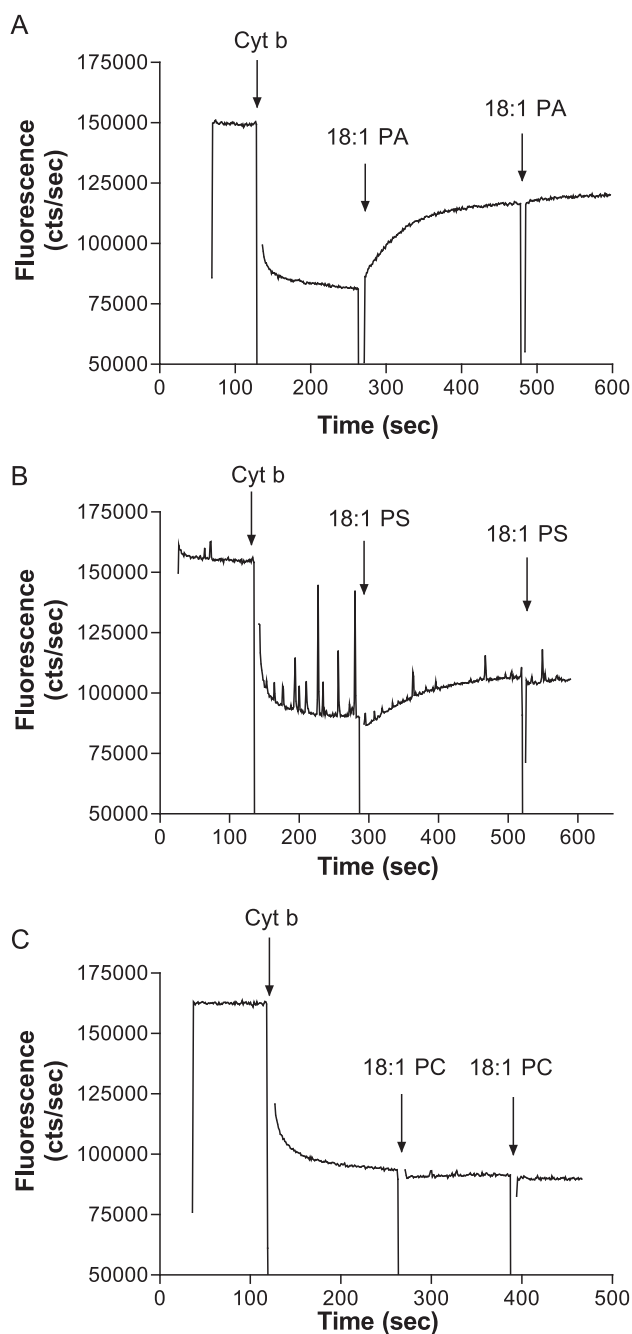


Fig. 6. The effect of headgroup on phospholipid-mediated conformational changes in immunoaffinity-purified flavocytochrome *b*. To examine the specificity of PA for inducing conformational changes in flavocytochrome *b*, a variety of 18:1 lipids were evaluated for their effect on the CCB-mAb 44.1:Cyt *b* complex. (A and B) The relaxation in fluorescence quenching when the CCB-mAb 44.1:Cyt *b* complex is exposed to DOPA and DOPS, respectively. In contrast, no significant relaxation in fluorescence quenching is observed in similar studies conducted with DOPC (C), DOPE (D) or 18:1 DAG (E). Arrows indicate the addition of both Cyt *b* (30 nM final) and lipids (100  $\mu$ M additions) to the fluorescence cuvette containing CCB-mAb 44.1 (10 nM).

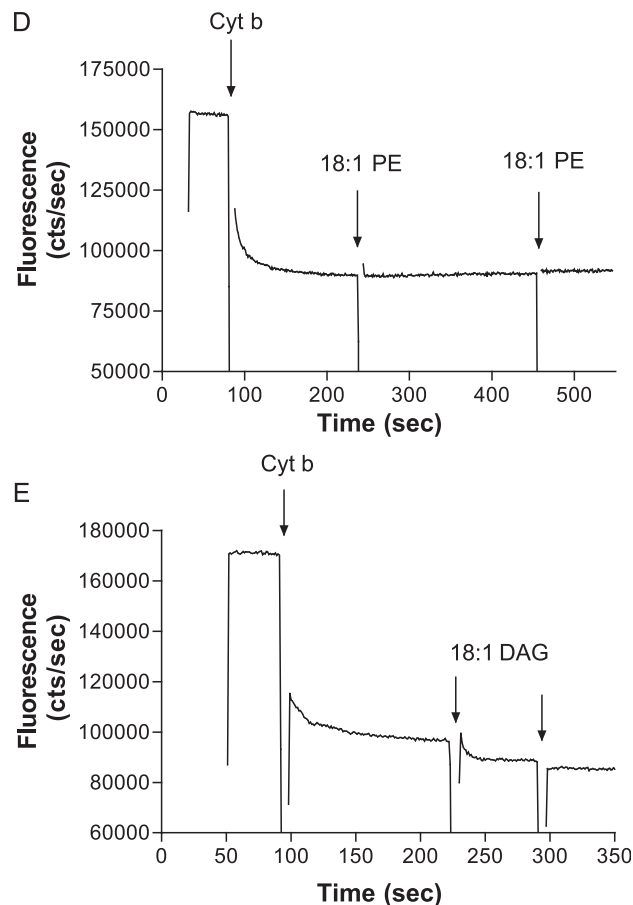


Fig. 6 (continued).

DOPA (data not shown). Table 1 summarizes results obtained with 8:0 and 18:1 DAG.

As described for the other lipids and amphiphiles examined (see Figs. 3 and 5), control experiments conducted with DOPS, DOPC, DOPE and DAG species similarly ruled out a trivial explanation for the observed results obtained in our energy transfer measurements (data not shown). Such results demonstrate the specificity of particular phospholipids for inducing structural rearrangements in detergent-solubilized flavocytochrome *b*, with long-chain PA species causing the most dramatic relaxation in fluorescence quenching under our assay conditions.

#### 4. Discussion

##### 4.1. CCB-mAb 44.1 as a probe for RET studies with flavocytochrome *b*

Cascade Blue acetyl azide is an amine-reactive, fluorescent compound that has a relatively high extinction coefficient and an emission spectrum with optimal overlap of the Cyt *b* Soret absorbance band. Using cytochrome *c* as a test case, the utility of CCB as a fluorescence donor for analyzing the structure and conformational dynamics of

heme-containing proteins by RET methods was previously demonstrated [36]. Initial efforts to apply such methods for the structure analysis of flavocytochrome *b* involved the generation of a CCB-labeled WGA conjugate which specifically bound the Cyt *b* N-linked glycan moieties. This system was used to demonstrate that detergent-solubilized Cyt *b* undergoes significant conformational changes in the presence of the anionic amphiphiles LDS and AA [26].

In the present study, we have extended results obtained with the CCB-WGA conjugate by labeling the Cyt *b*-specific, epitope-mapped mAb 44.1 [31] with CCB and examining a panel of amphiphiles and phospholipids for the ability to induce conformational changes in detergent-solubilized flavocytochrome *b*. Additionally, the Cyt *b* sample used in the present RET studies was generated by a recently described immunoaffinity purification method [9] that results in a more highly purified preparation than previously employed. CCB-mAb 44.1 bound to Cyt *b* with high specificity and affinity, providing a more defined probe for conducting energy transfer studies than the WGA conjugate.

Although a valuable reagent for demonstrating lipid and amphiphile-induced conformational changes in Cyt *b*, obtaining accurate distance measurements from the mAb 44.1 epitope to the Cyt *b* heme prosthetic groups by our current RET measurements is complicated by the fact that we have not precisely identified the specific mAb 44.1 residues labeled by CCB. Since acetyl azide compounds have been shown to selectively modify the N-termini of monoclonal IgG molecules under neutral pH conditions [29], current efforts are being directed at the generation of Fab fragments from various Cyt *b*-specific, epitope-mapped monoclonal antibodies, selectively labeled with CCB at their N-termini, as highly defined probes for estimating distances between antibody epitopes and the Cyt *b* heme prosthetic groups.

#### 4.2. The anionic amphiphiles LDS and AA modulate the conformation of flavocytochrome *b*

The anionic amphiphiles LDS and AA have long been employed to promote activation of the NADPH oxidase complex in *in vitro* assays of superoxide production [33,34]. RET measurements conducted in this study demonstrated the ability of LDS and AA to directly modulate the conformation of detergent-solubilized flavocytochrome *b* when introduced at levels where maximum activation of the NADPH oxidase complex is observed *in vitro*. The selectivity of these agents is further supported by the inability of the irrelevant anionic amphiphile deoxycholate or AA-ME to induce the dramatic relaxation of fluorescence quenching. These results are in accordance with a growing body of literature [25,26,37,38] supporting the contention that such anionic amphiphiles induce structural rearrangements in flavocytochrome *b* relevant to activation of the NADPH oxidase complex. From a structural perspective, it

is of interest to highlight a recent study by our group using CCB-labeled WGA that demonstrated a similar profile of relaxation of fluorescence quenching upon exposure to AA and LDS [26]. Since WGA binds the extracellular N-linked glycan moieties on gp91<sup>phox</sup> while mAb 44.1 recognizes an epitope residing on the cytoplasmic portion of p22<sup>phox</sup>, the energy transfer studies suggest that Cyt *b* conformational changes are both substantial and global in nature. Combined with observations implicating PLA<sub>2</sub>-generated AA as an *in vivo* regulator of superoxide generation by the NADPH oxidase complex [39], the above data support the hypothesis that AA modulates the conformation of flavocytochrome *b* in a physiologically relevant manner to promote superoxide production.

#### 4.3. Anionic phospholipids modulate the conformation of flavocytochrome *b*

The role of particular phospholipids in facilitating a catalytically active state of the NADPH oxidase complex has received considerable attention [4,10,20,35,40,41]. In the present study we demonstrate, for the first time, that both PA and phosphatidylserine are capable of directly modulating the conformation of flavocytochrome *b*. The long-chain, unsaturated phospholipid DOPA was observed to induce structural changes in DDM-solubilized Cyt *b* to a similar degree as AA, and appeared to be a more potent agent, as lower concentrations of DOPA were required to saturate the observed fluorescence relaxation. The anionic phospholipid DOPS also induced structural changes in DDM-solubilized Cyt *b*, although to a lesser extent than DOPA or AA. The relaxation induced by DOPA and DOPS was observed to be a kinetically slower process than observed for LDS, AA and short-chain PA species. These results might indicate a slower on-rate for binding of 18:1 phospholipids or may simply indicate that the 18:1 phospholipids require a longer period of time to disperse into Cyt *b*-containing DDM micelles.

The ability to induce such conformational changes in Cyt *b* appears to be mediated, in part, by an anionic lipid headgroup, as uncharged phospholipids of identical acyl chain composition were unable to produce the same effect. This behavior is consistent with the observed requirement for the anionic carboxylate group of AA for inducing conformational changes in flavocytochrome *b* (the neutral derivative AA-ME is inactive; [25,26]) and suggests charge to be an important criteria for association of lipid with flavocytochrome *b*. Consideration of both the lipid composition of neutrophil membranes [42] and the rapid activation of phospholipase D following cell stimulation [43] makes the ability of DOPA to potentially induce structural rearrangement in DDM-solubilized Cyt *b* of particular interest. It is also important to note that the 18:1 acyl chain (found in DOPA) has been demonstrated to be a highly abundant constituent of neutrophil membrane phospholipids [42]. Thus, it appears that long-chain, unsaturated PA species

must be considered as potential physiologically relevant regulators of Cyt *b* conformation. In the neutrophil membrane, anionic lipids might serve to support conformations of Cyt *b* that allow association with oxidase cytosolic factors and/or allow efficient electron transfer. Although a difficult task, it will be of particular interest to directly demonstrate specific binding of anionic phospholipids and amphiphiles to Cyt *b* and to characterize the structural features of this integral membrane protein that mediate such binding. Preliminary studies demonstrating the ability of AA-ME to diminish PA-induced conformational changes in DDM-solubilized Cyt *b* raise the possibility that diverse lipids share a common or partially overlapping binding site on Cyt *b*.

In light of our current observations, it is also important to highlight previous studies demonstrating that PA and DAG both activate superoxide production by directly interacting with components of the NADPH oxidase complex [20]. Examination of DAG species by RET in the present study indicated no ability of this lipid to induce conformational changes in Cyt *b* or to potentiate the ability of DOPA to induce structural rearrangements. These results do not rule out the possibility that DAG specifically associates with Cyt *b* to serve some sort of a regulatory role in superoxide production.

#### 4.4. Regulation of assembly and activation of the phagocyte NADPH oxidase complex by lipid second messengers

Activation of phagocytes by a variety of different stimuli results in the enzymatic remodeling of membrane phospholipids and generation of second messenger species including AA, DAG and PA [12]. A number of studies have demonstrated both activation of superoxide production in a time course that parallels the generation of the above molecules and the ability of such lipid second messengers to directly regulate assembly and activation of the NADPH oxidase complex. The present study demonstrates the ability of the second messenger lipids AA and PA to modulate the conformation of the catalytic component of the NADPH oxidase complex, raising the possibility that flavocytochrome *b* serves as a physiologically relevant target for regulation by these lipids *in vivo*. The complexity of lipid-induced activation of superoxide production is highlighted by studies demonstrating the ability of second messenger lipids to directly act on multiple components of the NADPH oxidase complex including flavocytochrome *b* (Refs. 25,26 and this study), p47<sup>phox</sup> [14–18] and Rac-GDI [13]. The role of second messenger lipids in regulation of superoxide production is further complicated by the ability of these species to activate protein kinases responsible for phosphorylation of oxidase components [12]. Complex regulation involving a requirement for the simultaneous interaction of second messenger lipids with both protein kinases and multiple components of the NADPH oxidase complex might be anticipated in light of the strict spatial and temporal

requirements for superoxide generation in a productive immune response.

#### Acknowledgements

The authors gratefully acknowledge Connie Lord for the preparation of mAb 44.1 hybridoma culture supernatant and Jeannie Gripenroeg for the preparation of neutrophil plasma membrane fractions.

This work was supported by an Arthritis Foundation Postdoctoral Fellowship (to R.M.T.), American Heart Association SDG Award 30156N (to J.B.B.), March of Dimes Research Foundation, grant #1-FY02-191 (to L.C.M.) and by United States Public Health Service Grant R01 AI 26711 (to A.J.J.).

#### References

- [1] J.T. Curnette, M.C. Dinauer, in: G. Stamatoyannopoulos, et al. (Eds.), *The Molecular Basis of Phagocyte Blood Diseases*, Saunders, Philadelphia, 2001, pp. 539–563.
- [2] S.J. Weiss, Tissue destruction by neutrophils, *N. Engl. J. Med.* 320 (1989) 365–376.
- [3] P.V. Vignais, The superoxide-generating NADPH oxidase: structural aspects and activation mechanism, *Cell. Mol. Life Sci.* 59 (2002) 1428–1459.
- [4] V. Koshkin, E. Pick, Generation of superoxide by purified and re-lipidated cytochrome *b*<sub>559</sub> in the absence of cytosolic activators, *FEBS Lett.* 327 (1993) 57–62.
- [5] Y. Nisimoto, H. Otsuka-Murakami, J.D. Lambeth, Reconstitution of flavin-depleted neutrophil flavocytochrome *b*<sub>558</sub> with 8-mercapto-FAD and characterization of the flavin-reconstituted enzyme, *J. Biol. Chem.* 270 (1995) 16428–16434.
- [6] J. Doussiere, G. Buzenet, P.V. Vignais, Photoaffinity labeling and photoinactivation of the O<sub>2</sub><sup>-</sup> generating oxidase of neutrophils by an azido derivative of FAD, *Biochemistry* 34 (1995) 1760–1770.
- [7] A.R. Cross, J. Rae, J.T. Curnutte, Cytochrome *b*<sub>245</sub> of the neutrophil superoxide-generating system contains two nonidentical hemes, *J. Biol. Chem.* 270 (1995) 17075–17077.
- [8] J. Doussiere, J. Gaillard, P.V. Vignais, The heme component of the neutrophil NADPH oxidase complex is a target for arylidonium compounds, *Biochemistry* 38 (1999) 3694–3703.
- [9] R.M. Taylor, J.B. Burritt, T.R. Foubert, M.A. Snodgrass, K.C. Stone, D. Baniulis, J.M. Gripenroeg, C. Lord, A.J. Jesaitis, Single-step immunoaffinity purification and characterization of dodecylmaltoside-solubilized human neutrophil flavocytochrome *b*, *Biochim. Biophys. Acta* 1612 (2003) 65–75.
- [10] V. Koshkin, E. Pick, Superoxide production by cytochrome *b*<sub>559</sub>: mechanism of cytosol-independent activation, *FEBS Lett.* 338 (1994) 285–289.
- [11] B.M. Babior, NADPH oxidase: an update, *Blood* 93 (1999) 1464–1467.
- [12] L.C. McPhail, K.A. Waite, D.B. Regier, J.B. Nixon, D. Quallitotene-Mann, W.-X. Zhang, R. Wallin, S. Sergeant, A novel protein kinase target for the lipid second messenger phosphatidic acid, *Biochim. Biophys. Acta* 1439 (1999) 277–290.
- [13] T.-H. Chuang, B.P. Bohl, G.M. Bokoch, Biologically active lipids are regulators of Rac-GDI complexation, *J. Biol. Chem.* 268 (1993) 26206–26211.
- [14] S.D. Swain, S.L. Helgersson, A.R. Davis, L.K. Nelson, M.T. Quinn, Analysis of activation-induced conformational changes in p47<sup>phox</sup>



- using tryptophan fluorescence spectroscopy, *J. Biol. Chem.* 272 (1997) 29502–29510.
- [15] H.-S. Park, J.-W. Park, Fluorescent labeling of the leukocyte NADPH oxidase subunit p47<sup>phox</sup>: evidence for amphiphile-induced conformational changes, *Arch. Biochem. Biophys.* 360 (1998) 165–172.
- [16] H.-S. Park, J.-W. Park, Conformational changes of the leukocyte NADPH oxidase subunit p47<sup>phox</sup> during activation studied through its intrinsic fluorescence, *Biochim. Biophys. Acta* 1387 (1998) 406–414.
- [17] H. Sumimoto, Y. Kage, H. Nunoi, H. Sasaki, T. Nose, Y. Fukumaki, M. Ohno, S. Minakami, K. Takeshige, Role of Src homology 3 domains in assembly and activation of the phagocyte NADPH oxidase, *Proc. Natl. Acad. Sci.* 91 (1994) 5345–5349.
- [18] A. Shiose, H. Sumimoto, Arachidonic acid and phosphorylation synergistically induce a conformational change of p47<sup>phox</sup> to activate the phagocyte NADPH oxidase, *J. Biol. Chem.* 275 (2000) 13793–13801.
- [19] J.-W. Park, Phosphatidic acid-induced translocation of cytosolic components in a cell-free system of NADPH oxidase: mechanism of activation and effect of diacylglycerol, *Biochem. Biophys. Res. Commun.* 229 (1996) 758–763.
- [20] A. Palicz, T.R. Foubert, A.J. Jesaitis, L. Marodi, L.C. McPhail, Phosphatidic acid and diacylglycerol directly activate NADPH oxidase by interacting with enzyme components, *J. Biol. Chem.* 276 (2001) 3090–3097.
- [21] R.W. Erickson, P. Langel-Peveri, A.E. Traynor-Kaplan, P.G. Heyworth, J.T. Curnutte, Activation of human neutrophil NADPH oxidase by phosphatidic acid or diacylglycerol in a cell-free system, *J. Biol. Chem.* 274 (1999) 22243–22250.
- [22] N. Alloul, Y. Gorzalczany, M. Itan, N. Sigal, E. Pick, Activation of the superoxide-generating NADPH oxidase by chimeric proteins consisting of segments of the cytosolic component p67<sup>phox</sup> and the small GTPase Rac1, *Biochemistry* 40 (2001) 14557–14566.
- [23] Y. Gorzalczany, N. Alloul, N. Sigal, C. Weinbaum, E. Pick, A prenylated p67<sup>phox</sup>-Rac1 chimera elicits NADPH-dependent superoxide production by phagocyte membranes in the absence of an activator and of p47<sup>phox</sup>, *J. Biol. Chem.* 277 (2002) 18605–18610.
- [24] P. Bellavite, F. Corso, S. Dusi, M. Grzeskowiak, V. Della-Bianca, F. Rossi, Activation of NADPH oxidase-dependent superoxide production in plasma membrane extracts of pig neutrophils by phosphatidic acid, *J. Biol. Chem.* 263 (1988) 8210–8214.
- [25] J. Doussiere, J. Gaillard, P.V. Vignais, Electron transfer across the O<sub>2</sub><sup>-</sup> generating flavocytochrome *b* of neutrophils. Evidence for a transition from a low-spin state to a high-spin state of the heme iron component, *Biochemistry* 35 (1996) 13400–13410.
- [26] T.R. Foubert, J.B. Burritt, R.M. Taylor, A.J. Jesaitis, Structural changes are induced in human neutrophil cytochrome *b* by NADPH oxidase activators, LDS, SDS and arachidonate: intermolecular resonance energy transfer between trisulfonyl-pyrenyl-wheat germ agglutinin and cytochrome *b*<sub>558</sub>, *Biochim. Biophys. Acta* 1567 (2002) 221–231.
- [27] C.G. dos Remedios, P.D. Moens, Fluorescence resonance energy transfer spectroscopy as a reliable “ruler” for measuring structural changes in proteins: dispelling the problem of the unknown orientation factor, *J. Struct. Biol.* 115 (1995) 175–185.
- [28] T. Heyduk, Measuring protein conformational changes by FRET/LRET, *Curr. Opin. Biotechnol.* 13 (2002) 292–296.
- [29] H. Kaplan, B.G. Long, N.M. Young, Chemical properties of functional groups of mouse immunoglobins of the IgA, IgG2a, and IgM classes, *Biochemistry* 19 (1980) 2821–2827.
- [30] R. Lutter, M.L.J. van Schaik, R. van Zwieten, R. Wever, D. Roos, M.N. Hamers, Purification and partial characterization of the *b*-type cytochrome from polymorphonuclear leukocytes, *J. Biol. Chem.* 260 (1985) 2237–2244.
- [31] J.B. Burritt, S.C. Busse, D. Gizachew, D.W. Siemsen, M.T. Quinn, C.W. Bond, E.A. Dratz, A.J. Jesaitis, Antibody imprint of a membrane protein surface, *J. Biol. Chem.* 273 (1998) 24847–24852.
- [32] J.E. Whitaker, R.P. Haugland, P.L. Moore, P.C. Hewitt, M. Reese, R.P. Haugland, Cascade Blue derivatives: water soluble, reactive, blue emission dyes evaluated as fluorescent labels and tracers, *Anal. Biochem.* 198 (1991) 119–130.
- [33] Y. Bromberg, E. Pick, Unsaturated fatty acids stimulate NADPH-dependent superoxide production by cell-free system derived from macrophages, *Cell. Immunol.* 88 (1984) 213–221.
- [34] Y. Bromberg, E. Pick, Activation of NADPH-dependent superoxide production in a cell-free system by sodium dodecyl sulfate, *J. Biol. Chem.* 260 (1985) 13539–13545.
- [35] D. Qualliotone-Mann, D.E. Agwu, M.D. Ellenburg, C.E. McCall, L.C. McPhail, Phosphatidic acid and diacylglycerol synergize in a cell-free system for activation of NADPH oxidase from human neutrophils, *J. Biol. Chem.* 268 (1993) 23843–23849.
- [36] R.M. Taylor, B. Lin, T.R. Foubert, J.B. Burritt, J. Sunner, A.J. Jesaitis, Cascade Blue as a donor for resonance energy transfer studies of heme-containing proteins, *Anal. Biochem.* 302 (2002) 19–27.
- [37] J. Doussiere, R. Bouzidi, A. Poinas, J. Gaillard, P.V. Vignais, Kinetic study of the activation of the neutrophil oxidase by arachidonic acid. Antagonistic effects of arachidonic acid and phenylarsine oxide, *Biochemistry* 38 (1999) 16394–16406.
- [38] M.-H. Paclet, A.W. Coleman, S. Vergnaud, F. Morel, p67-phox-mediated NADPH oxidase assembly: imaging of cytochrome *b*<sub>558</sub> liposomes by atomic force microscopy, *Biochemistry* 39 (2000) 9302–9310.
- [39] R. Dana, T.L. Leto, H.L. Malech, R. Levy, Essential requirement of cytosolic phospholipase A<sub>2</sub> for activation of the phagocyte NADPH oxidase, *J. Biol. Chem.* 273 (1998) 441–445.
- [40] S. Shpungin, I. Dotan, A. Abo, E. Pick, Activation of the superoxide forming NADPH oxidase in a cell-free system by sodium dodecyl sulfate, *J. Biol. Chem.* 264 (1989) 9195–9203.
- [41] M. Tamura, T. Tamura, S.R. Tyagi, J.D. Lambeth, The superoxide-generating respiratory burst oxidase of human neutrophil plasma membrane, *J. Biol. Chem.* 263 (1988) 17621–17626.
- [42] S. Cockcroft, D. Allan, The fatty acid composition of phosphoinositol, phosphatidate and 1,2-diacylglycerol in stimulated human neutrophils, *Biochem. J.* 222 (1984) 557–559.
- [43] D.E. Agwu, L.C. McPhail, R.L. Wykle, C.E. McCall, Mass determination of receptor-mediated accumulation of phosphatidate and diglycerides in human neutrophils measured by Coomassie blue staining and densitometry, *Biochem. Biophys. Res. Commun.* 159 (1989) 79–86.